Investigation on solar humidification dehumidification water desalination system using a closed-air cycle

A. S. A. Mohamed [a,b,*], , Abanob G. Shahdy [c], M. Salem Ahmed [a]

[a] Mechanical Department, Faculty of Technology and Education, Sohag University, Sohag 82524, Egypt
[b] High Institute for Engineering and Technology, Sohag, Egypt
[c] Industrial Secondary School, Sohag, Egypt

* Corresponding author E-mail address: ahmedquse2000@yahoo.com (A. S. A. Mohamed).

Abstract

This research presents a theoretical and experimental study of a solar humidification dehumidification water desalination system based on a closed-air cycle. The results show that productivity enhances with increasing air flow-rate while the gain output ratio decreases. The gain output ratio and productivity improve with raising the temperature of water. The average value of gain output ratio is 0.71, 0.74, 0.78, and 0.81, and productivity is 1.46 kg/h, 2.59 kg/h, 4.40 kg/h, and 6.99 kg/h at water temperatures of 40 °C, 50 °C, 60 °C, and 70 °C, respectively. The maximum gain output ratio of 0.86 is recorded at water to air mass flow-rate ratio of 5. Increasing the cooling water flow-rate has a positive effect on both productivity and gain output ratio. Moreover, The results indicate that the fresh water cost is 0.012 $/L. Finally, a good agreement is noted between the theoretical and experimental results.

Keywords: Water desalination; Humidification-dehumidification; Experimental evaluation; Solar energy; productivity.

Nomenclature

a	Instrument accuracy
A	Air- water exchange area, m^2/m^3
Cp	Specific heat, J/kg K
D_{h1}	Hydraulic diameter of air flow, m
D_{h2}	Hydraulic diameter of water flow, m
g	Gravitational acceleration, m/s^2
G	Gas mass velocity, kg/m^2 s
h	Heat transfer coefficient at air water interface, W/m^2 K
h_c	Heat transfer coefficient of condensate film, W/m^2 K
h_e	Heat transfer coefficient at water condenser inside wall interface, W/m^2 K
h_{fg}	Evaporation latent heat, J/kg
H	Enthalpy, kJ/kg
k	Thermal conductivity, W/m K
K	Mass transfer cofficient at air water interface, kg/m^2 s
L	Liquid mass velocity, kg/m^2 s
$\dot{m}$	Mass flow-rate, kg/s
N	Number of rows of horizontal tubes in the condenser, dimensionless
P	Pressure, pa
P_t	longitudinal pitch, m
P_l	Transverse pitch, m
Pr	Prandtl number
$\dot{Q}$	Heat transfer rate, Kw
Re	Reynolds number
T	Temperature, K
T_i	Temperature at air water interface, K
u	Standard uncertainty
U	Condenser overall heat transfer coefficient, W/m^2 K
V	Volume, m^3

Greek symbols

δ	Tube wall thickness, m
η	Efficiency
μ	Dynamic viscosity, Ns/m^2
ρ	Water density, kg/m^3
ω	Absolute humidity of air, kg vapor/kg dry air

Subscripts

a	Air
atm	Atmosphere
c	Condenser
cw	Cooling water
dh	Dehumidifier
Fw	Fresh-water
h	Humidifier

in	Inlet
o	Outlet
P	Packing
sat	Saturation condition
S	Solar collector
w	Water
W	Wall

Abbreviations

GOR	Gain output ratio
HDH	Humidification-dehumidification
MR	Mass flow-rate ratio

1. Introduction

In addition to the traditional sources such as the Nile River and the underground water, Egypt needs to find new sources of fresh water to provide the increasing demand on the fresh water for drinking, agriculture, industry, and desert reclamation. The Nile River and the underground water are not considered a suitable solution for providing water to the Egyptian desert. This is because the Nile River needs pipelines or channels and dams building that must be implemented with high capacity and accuracy. Meanwhile, the underground water that is expected to be enormous, need to examine its sustainability capacity and its suitability for different applications (Nafey et al., 2004a).

The essential geographical location of Egypt (as it overlooks distinct water borders, including: the Mediterranean and the Red Sea) is one of the most important reasons that researchers think about desalination of salt water (seawater) as a solution to obtain fresh water. Desalination is the process of reducing the percentage of salts dissolved in seawater to produce usable water. In general, seawater is desalinated by either evaporating water or separating fresh water using a membrane. Recently considered desalination methods using evaporation of water is humidification-dehumidification (HDH) water desalination technique. This technique has many advantages that made it the subject of study in many researches in the last period, such as the simplicity of construction, energy use at low temperature, and low cost of construction and maintenance. HDH water desalination processes operate with atmospheric pressure; so it consumes little of mechanical energy only for air and water circulation (Yildirim and Solmuş, 2014, Patel et al., 2014).

HDH desalination system consumes great heat energy in order to separate the salts from seawater. Initially, traditional energy sources (fossil fuels) were used to provide energy for desalination systems, where 10,000 tons of fossil fuels are consumed annually to produce 1000 m^3 per day of fresh water (Kalogirou, 2005). High consumption of traditional energy has caused

increasing concerns regarding greenhouse gas emissions and limited resources of fossil fuels, threatening the sustainable development process. Therefore, switching to renewable sources has become a growing trend in desalination systems. Solar energy appears to be the most viable solution to this problem, since it is reliably abundant in regions with low levels of fresh water (Zhang et al., 2018).

Solar energy presented in different types of solar collectors is used for heating water or air or both in HDH systems. For example, the water heating using the solar collector (evacuated tube) is applied in two different studies of HDH systems (Kabeel et al., 2014, Hamed et al., 2015). These systems were carried out using open and closed cycles for water and air, respectively. Cellulous papers were used in humidifier tower for increasing the direct contact area between the air and the water. A special design of condenser was used to heat exchange between liquid and gas in the dehumidifier chamber. The results revealed that the fresh water productivity is 23.6 L/h and 5.5 L/h for the first and second system, respectively.

To heat the air and water together, Yildirim and Solmuş (2014) used a solar collector (flat plate) in their HDH system. The results show that water heating has proven effective in producing the fresh water compared to air heating.

Wu et al. (2017) used solar collector (direct concentrated) device as a heat source for humidification process in their HDH water desalination system. They used three-stage cylindrical Fresnel lens as a solar concentrator in addition to a heat recovery stage. The results indicated that the best gain output ratio (GOR) and fresh water productivity are 2.1 and 3.4 kg/h, respectively with the average solar irradiation of 867 W/m^2.

Two types of solar collector are used by Nafey et al. (2004a), Nafey et al. (2004b) as a heating source for air and water in their experimental investigations of HDH system. First, a parabolic solar collector (concentrating collector) is used as a reflector frame for heating the seawater. Second, a solar collector (flat plate) covered by one layer of glass is used to heating the air. They found that the freshwater productivity of the system is greatly affected by the temperature of the hot water entering the humidifier, the cooling water flow-rate in the dehumidifier, the air flow-rate, and the solar irradiation. Moreover, the ambient temperature and wind speed had a weak effect on the fresh water productivity. They also developed the mathematical correlation to predict fresh water production with different operating conditions. The mathematical correlation showed acceptable results with an error ±6%. They also found that the area of solar water collector has a clear impact on the productivity of fresh water compared to the area of the solar air collector.

Fouda et al. (2018) presented a performance analysis of HDH water desalination system powered by solar energy using three stages; single, double, and modified double stages for hot and

humid countries. They found that using solar collectors for water and air heating greatly enhanced the performance of the desalination system. In addition, they found that the proposed MDS system has the best performance and the highest productivity can reach to 350 L/day with GOR of 1.63.

Mohamed et al. (2020) presented an experimental study for HDH water desalination system powered by solar energy represented in heating the water before entering the humidifier chamber using solar collector (evacuated tube). The system is installed based on a closed air cycle and open water cycle. In this system, structure-packing materials (Cellulose paper) are used for increasing the heat transfer area between the air and hot water inside the humidifier, and a heat exchanger (finned tube) is used to condensate the water vapor inside the dehumidifier. The experimental results were used to confirm the theoretical model. They found that the average fresh water productivity is about 2.45 L/h and the cost of producing one liter is about 0.047 US$. The results showed a good agreement between the experimental results and theoretical values.

The solar energy can be used for assisting some other energy sources in HDH systems which called hybrid energy as used by Xu et al. (2018). They used solar energy for assisting heat pump cycle in their experimental HDH system. The hybrid unit consists of heat pump cycle, in addition to humidifier chamber, fan and storage tank. The heat pump cycle works with 134a as a working fluid, and a honeycomb packing material is placed inside the humidifier. They found that the maximum GOR of the system is 1.24, and the highest water productivity is 12.38 kg/kWh. The cost of productivity is 29.8 $/ton, assuming that 20 years is the lifetime.

Gao et al. (2008) used the mechanical vapor compression pump for driving a new type of desalination system based on HDH technique. Initially, the air is heated (using solar collector) then humidified during the humidification process, and followed by pre-cooling in the condenser then cooled in evaporator to produce the fresh water. The heat pump condenser heats the air at the night or the condition of sunlight is low. To recover the lost energy, the seawater is preheated initially as it passes into the condenser. The results revealed that the maximum fresh water productivity is 60 liter per day with less electric power that is 500 W (compressor rated power).

Hou and Zhang (2008) studied hybrid solar water desalination system using multi-effect HDH. In this unit, a solar collector (evacuated tube) was used as a source of heating. The results show that reusing the rejected water in this system increases GOR by 2 to 3. In another endeavor, Sharshir et al. (2016) studied a hybrid solar water desalination system comprising solar stills and HDH technique. In this system, the warm water outlet from the humidifier is directed to feed solar stills to conserve the energy. They found that the efficiency of the solar still is 90%, and GOR of the system increases about 50% due to re-use the warm water outlet from the humidifier. Moreover, the solar still production in this system has been doubled compared to the conventional solar still. The cost

production of fresh water by conventional, HDH, and hybrid water desalination system are 0.049 $/L, 0.058 $/L and 0.034 $/L, respectively.

The current work presents the results of study for HDH seawater desalination system using a closed-air cycle powered by solar energy. Theoretical and experimental investigations have been conducted for evaluating the system performance. Finally, the study presents an economic evaluation of water production.

2. Experimental-Setup

2.1. System description

The current work presents an experimental evaluation for HDH water desalination system using a closed cycle for air streams. The system operates according to three cycles, the air cycle, the hot seawater cycle, and the cold water cycle. Figure 1 and Fig. 2 showed a photograph and a schematic diagram for the experimental-setup, respectively. HDH desalination system consists of humidifier chamber, dehumidifier chamber, solar water-collector, water pump, air fan, and auxiliary heater.

The air cycle begins as the air enters the humidifier from below to exchange heat and moisture with hot seawater sprayed from the top. Then, the hot and humid air comes out from the humidifier and goes to the dehumidifier to be cooled in order to obtain the fresh water. Finally, the dehumidified air returns to the humidifier to complete the cycle and begin a new cycle. For hot seawater cycle, seawater is heated by an evacuated tube solar water-collector, then stored in an insulated tank (40 cm × 50 cm × 90 cm) which including an auxiliary electric heater to maintain a constant operating seawater temperature. Then, the hot water is withdrawn from the tank by a pump (0.5 hp) to be sprayed over the packing material in the humidifier. The brine water collected below the humidifier chamber is returned back to the solar water-collector to be reheated and used in a new cycle, as shown in Fig. 2. In cooling water cycle, the cooling water is passed in a condenser to make its surface temperature less than the dew point temperature of hot and humid air, with the aim of starting the condensation process on the surface of the condenser and thus collecting the fresh water at the bottom, as shown in Fig. 2.

The humidifier chamber is made from galvanized steel (thickness=0.8 mm). Its height, length, and width are 120 cm, 40 cm, and 50 cm, respectively. In the humidifier, cellulose paper with specific area of 300 m^2/m^3 is used as an area of heat and mass transfer. To decrease the energy loss, the humidifier is insulated by 3 cm glass-wool layer (k = 0.036 W/m K). The dehumidifier is 100 cm high, 32 cm long, 32 cm wide, and 1 mm thick. Finned tube heat exchanger is placed inside the

humidifier to be a medium for the exchange of heat and mass between the cooling water and the hot and humid air. The source of heating energy for the HDH water desalination system is represented by the solar water-collector (evacuated tube).

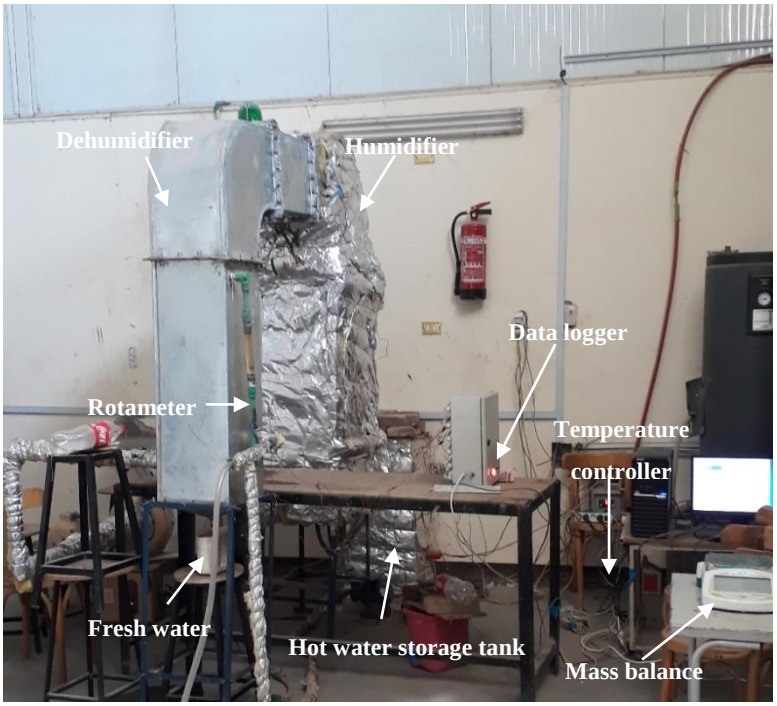

Fig. 1. Photograph of experimental setup.

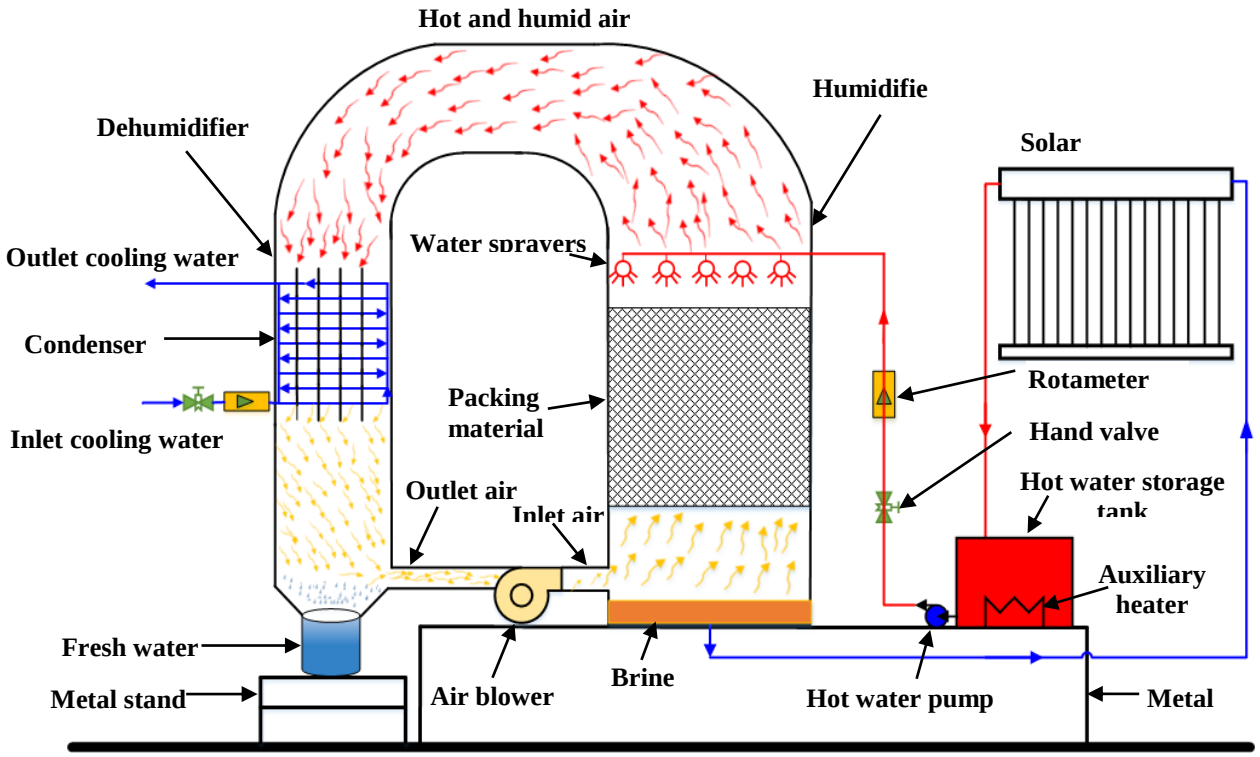

Fig. 2. Schematic diagram of experimental setup.

2.2. Measured data

To investigate the performance of HDH desalination unit, several parameters are measured through the implementation of the experiments. The parameters include temperatures of air before and after the humidifier and dehumidifier chambers, and the temperatures of water before and after the humidifier and dehumidifier chambers. The mass flow-rates of air and hot seawater before the humidifier, and mass flow-rate of cooling water before dehumidifier also have been recorded. Besides, the solar intensity and freshwater produced are recorded.

The air/water temperatures in HDH desalination system are measured by thermocouples (type-K) connected to data logger unit (±0.5°C). To determine the air flow-rate, the air-velocity is recorded using wireless anemometer (0.4-30m/s and accuracy of ±3%). Two-rotameters (0.5-2m^3/h and accuracy of ±4%) are used to measure the water flow-rates. The first one is used to measure the mass flow-rate of seawater inlet to humidifier, and another used to record the mass flow-rate of cooling-water inlet to dehumidifier. In addition, the solar intensity is measured by solarimeter with accuracy of ±1W/m^2. Finally, the freshwater produced is measured by collecting during the experiment time and then weighing the fresh water using a mass balance with accuracy of 0.1g.

2.3. Experimental uncertainty analysis

The accuracy of the results in the experiments is extremely important. Therefore, an uncertainty analysis of the experimental results and the devices used in the experiments has been performed. The random and systematic errors are the important factors, which affect in the accuracy of measurement and thus the experimental results. The random error varies depending on the skills and capabilities of the experimental work, while the systematic error depends on the limitation and the accuracy of the measurement devices. In this study, all the data collected within the experimental work are taken from digital devices with known accuracy. Subsequently, standard uncertainty is expressed and given in equation (1) (Rahbar and Esfahani, 2012, Srithar et al., 2018). Finally, the standard uncertainty of the measurement devices is illustrated in table 1.

$$u = \frac{a}{\sqrt{3}} \quad (1)$$

Where u standard uncertainty, a accuracy of the instrument.

Table 1
Standard uncertainty of the measurement devices.

Device	Accuracy	Amplitude	Uncertainty
Temperature (type-K)	±0.5°C	0-200°C	0.29°C
Anemometer	±3%	0.4-30m/s	1.73%
Rotameter	±4%	0.5-2m^3/h	2.31%
Solarimeter	±1W/m^2	0-5000W/m^2	0.58W/m^2
Mass balance	0.1g	0-4000g	0.05g

3. Heat and Mass Balance for Main Components

Heat and mass balance has been applied for the main system components such as humidifier, dehumidifier, and solar water-collector. Assumptions for the components balance include; HDH desalination system operates with steady state conditions; energy loss of HDH system is negligible; the pressure drop within HDH system is neglected; and the power of fan and pump is neglected compared with the solar heat required to HDH system. The heat and mass balance equations for the main components can be displayed as follows.

3.1. Heat and mass balance for humidifier

During the humidification process, heat and mass are exchanged between hot water and air. Inlet and outlet flow directions for the air and water at humidifier and dehumidifier chambers are illustrated in Fig. 3. Mass and energy balance Eq. (2) and Eq. (3) are obtained by applying the laws of the thermodynamics.

$$\dot{m}_{w,o,h} = \dot{m}_{w,in,h} - \dot{m}_{Fw} \quad (2)$$

$$\dot{m}_a \left(H_{a,o,h} - H_{a,in,h}\right) = \dot{m}_{w,in,h} H_{w,in,h} - \dot{m}_{w,o,h} H_{w,o,h} \quad (3)$$

Where $\dot{m}_{w,o,h}$ is mass flow-rate of water outlet from humidifier; $\dot{m}_{w,in,h}$ is mass flow-rate of water inlet to humidifier; $\dot{m}_{Fw}$ is mass flow-rate of freshwater produced; $\dot{m}_a$ is mass flow-rate of air; $H_{a,in,h}, H_{a,o,h}$ is enthalpy of air before and after humidifier; and $H_{w,in,h}, H_{w,o,h}$ is enthalpy of water before and after humidifier, respectively.

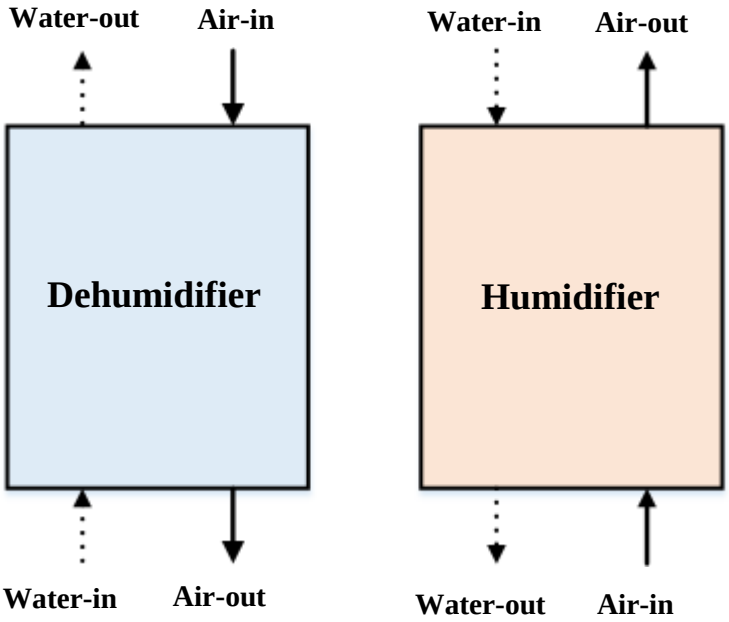

Fig. 3. Humidifier and dehumidier control volumes.

3.2. Heat and mass balance for dehumidifier

The process of heat and mass exchange takes place simultaneously inside the dehumidifier, which is similar to that inside the humidifier. Mass and energy balances for the dehumidifier are given by Eq. (4) and Eq. (5).

$$\dot{m}_{Fw} = \dot{m}_a\left(\omega_{a,in,dh} - \omega_{a,o,dh}\right) \quad (4)$$

$$\dot{m}_a\left(H_{a,in,dh} - H_{a,o,dh}\right) = \dot{m}_{cw}\left(H_{cw,o,c} - H_{cw,in,c}\right) + \dot{m}_{Fw}H_{Fw} \quad (5)$$

Where $\omega_{a,in,dh}, \omega_{a,o,dh}, H_{a,in,dh}, H_{a,o,dh}$ is moisture content and enthalpy of air before and after dehumidifier, respectively; $\dot{m}_{cw}$ is flow-rate of cooling-water; $H_{cw,in,c}, H_{cw,o,c}$ is enthalpy of cooling-water inlet to and outlet from condenser; and H_{Fw} is enthalpy of freshwater.

3.3. Energy balance for solar water-collector

The current HDH water desalination system is powerd by solar energy (Evacuated tube water-collector). Solar collector is single stream heat exchanger. The governing equations of single stream solar collector are reduced to Eq. (6).

$$\dot{Q}_S = \dot{m}_{w,in,h} Cp_w\left(T_{w,in,h} - T_{w,o,h}\right) \quad (6)$$

Where $\dot{Q}_S$ is the solar energy inlet to HDH desalination system; Cp_w is the specific heat of water; and $T_{w,in,h}, T_{w,o,h}$ is temperature of water inlet to and outlet from humidifier, respectively.

Property data for water and air have been obtained from the literature. The seawater and humid air properties are obtained by Conde, (2007), Sharqawy et al. (2010), respectively. Engineering Equation Solver (EES) is used to deal with the governing equations of heat and mass transfer process.

4. Performance Indices

HDH system performance has been demonstrated by some important parameters such as; productivity, gain output ratio (GOR), mass flow-rate ratio (MR), humidifier efficiency (η_h) and dehumidifier efficiency (η_{dh}). Therefore, each parameter has been defined to study, analyze, and evaluate HDH desalination system performance.

a. Productivity

The freshwater productivity is defined as water vapor content removed from air stream by the condenser in the dehumidifier chamber and can be calculated using Eq. (4).

b. Gain output ratio (GOR)

GOR is the ratio between evaporation latent heat of freshwater produced and total energy required to operate the system, and given by Eq. (7) (Kabeel et al., 2013).

$$\mathrm{GOR} = \frac{\dot{m}_{Fw} \times h_{fg}}{\dot{Q}_S} \tag{7}$$

Where h_{fg} latent heat of water vaporization.

c. Mass flow-rate ratio (MR)

MR is the mass flow-rate ratio between seawater and air before the humidifier, as given by Eq. (8) (Fouda et al., 2018).

$$\mathrm{MR} = \frac{\dot{m}_{w,in,h}}{\dot{m}_a} \tag{8}$$

d. Humidifier efficiency (η_h)

The humidifier efficiency is the ratio of actual changes in enthalpy/humidity ratio of the air to maximum change in enthalpy/humidity ratio of the air at the saturated temperature of outlet air, as given by Eq. (9) (Rajaseenivasan et al., 2016, Sharqawy et al., 2014, Zhang et al., 2018)

$$\eta_h = \left\{\frac{(H_{a,o,h} - H_{a,in,h})}{(H_{a,o,h,sat} - H_{a,in,h})}\right\} \text{or} \left\{\frac{(\omega_{a,o,h} - \omega_{a,in,h})}{(\omega_{a,o,h,sat} - \omega_{a,in,h})}\right\} \quad (9)$$

Where $H_{a,o,h,sat}$ is enthalpy of air outlet from humidifier at saturated air; $\omega_{a,in,h}, \omega_{a,o,h}$ is humidity ratio of air before and after humidifier; and $\omega_{a,o,h,sat}$ is the moisture content of air outlet from humidifier when the air is fully saturated.

e. Dehumidifier efficiency (η_{dh})

The efficiency of dehumidifier is the ratio between the real heat transfer rate and the maximum heat transfer rate taking place during the dehumidification process, or the ratio of actual change in the moisture content of the air across dehumidifier to maximum possible change of the moisture content in the air, which can be deduced from Eq. (10) (Kasamsetty and Raphael, 2018, Rajaseenivasan et al., 2016):

$$\eta_{dh} = \left\{\frac{(H_{a,in,dh} - H_{a,o,dh})}{(H_{a,in,dh} - H_{a,o,dh,sat})}\right\} \text{or} \left\{\frac{(\omega_{a,in,dh} - \omega_{a,o,dh})}{(\omega_{a,in,dh} - \omega_{a,o,dh,sat})}\right\} \quad (10)$$

Where $H_{a,o,dh,sat}$ is the enthalpy of air outlet from dehumidifier when air is fully saturated; and $\omega_{a,o,dh,sat}$ is specific humidity of air outlet from dehumidifier when the air is fully saturated.

5. Mathematical Model

The mathematical simulation represents the behavior of HDH water desalination system using the governing equations of heat and mass transfer in each component of the system. The mathematical description of the main components of HDH water desalination system is shown below.

5.1. The humidifier

Air blower forces the air through the packing material below the humidifier and hot seawater sprinkles on the packing material from the top. As a result, the heat and mass exchange occurs between the air and hot seawater. The mathematical model can be expressed by applying heat and mass balances on control volume with height Δx, as shown in Fig. 4.

Some assumptions were taken into consideration:

1- Humidification process is steady state conditions.
2- Hot water falling from the top is distributed regularly over the packing and hence, there is only a vertical gradient of temperature and humidity.
3- A very thin layer of saturated air exists between the water and the air streams.

Pursuant to the principle of mass balance, increasing the humidity ratio of the air leads to a decrease in the flow-rate of hot water, as shown in Eqs. (11,12).

$$G_{a,h}\frac{d\omega_{a,h}}{dx} = \frac{dL_w}{dx} \tag{11}$$

$$G_{a,h}\frac{d\omega_{a,h}}{dx} = k_{a,h}A_h\left(\omega_{sat,h} - \omega_{a,in,h}\right) \tag{12}$$

Eq. (12) can be rewritten as:

$$\frac{d\omega_{a,h}}{dx} = \frac{K_{a,h}A_h(\omega_{sat,h} - \omega_{a,in,h})}{G_{a,h}} \tag{13}$$

Where $G_{a,h}$ is the air mass velocity (kg/m^{2}s), L_w is the water mass velocity (kg/m^{2}s), $K_{a,h}$ is water interface mass transfer coefficient (kg/m^{2}s), A_h is the air water exchange area (m^2/m^3), $\omega_{sat,h}$ is saturation humidity of air water interface ($kg_{vapor}/kg_{dry\ air}$) and $\omega_{a,in,h}$ is the air humidity ratio before the humidifier ($kg_{vapor}/kg_{dry\ air}$).

Water phase heat balance; the heat energy that water losses is equal to the energy that is transferred to air water interface, as shown in Eq. (14).

$$L_w Cp_w dT_w = h_w A_h\left(T_{w,in,h} - T_{i,h}\right)dx \tag{14}$$

Eq. (14) can be rewritten as:

$$\frac{dT_w}{dx} = \frac{h_w A_h(T_{w,in,h} - T_{i,h})}{L_w Cp_w} \tag{15}$$

Where h_w is the heat transfer coefficient of water at air water interface (W/m^{2}K), $T_{i,h}$ is the temperature at air water interface (K).

Air phase heat balance; heat received by water air interface is equal to heat transmitted toward the air flow, as shown in Eq. (16).

$$G_{a,h}Cp_{a,h}dT_{a,h} = h_{a,h}A_h\left(T_{i,h} - T_{a,in,h}\right)dx \tag{16}$$

Eq. (16) can be reformulated as:

$$\frac{dT_{a,h}}{dx} = \frac{h_{a,h}A_h(T_{i,h} - T_{a,in,h})}{G_{a,h}Cp_{a,h}} \tag{17}$$

Where $Cp_{a,h}$ is specific heat of humid air (J/kgK), $h_{a,h}$ is heat transfer coefficient of air at the water air interface (W/m^{2}K).

The energy transfer from water to interface = energy transfer from interface to air (sensible and latent heat)

$$dq_w = dq_{a,sensible} + dq_{a,latent} \tag{18}$$

$$L_w A_h\left(T_{w,in,h} - T_{i,h}\right) = h_{a,h}A_h\left(T_{i,h} - T_{a,in,h}\right) + K_{a,h}A_h h_{fg}\left(\omega_{sat,h} - \omega_{a,in,h}\right) \tag{19}$$

Eq. (19) can be reformulated as:

$$\omega_{sat,h} = \frac{L_w A_h (T_{w,in,h} - T_{i,h}) + h_{a,h} A_h (T_{a,in,h} - T_{i,h})}{K_{a,h} A_h h_{fg}} + \omega_{a,in,h} \quad (20)$$

The saturation humidity ratio of the air ($\omega_{sat,h}$) also can be calculated by the terms of the saturation pressure of water vapor ($P_{sat,h}$), as shown in Eq. (21).

$$\omega_{sat,i,h} = 0.62198 \frac{P_{sat,h}}{P_{atm} - P_{sat,h}} \quad (21)$$

The saturation pressure of water vapor in the humidifier ($P_{sat,h}$) corresponding to a certain temperature can be calculated from (Amer et al., 2009).

$$P_{sat,h} = \mathrm{Exp}\left[\frac{-6096.938}{T_{i,h}} + 21.240964 - 2.71119 \times 10^{-2} T_{i,h} + 1.67395 \times 10^{-5} T_{i,h}^2 + 2.4335 \ln(T_{i,h})\right] \quad (22)$$

The mass transfer coefficient ($K_{a,h}$) and heat transfer coefficient for air and water inside humidifier ($h_{a,h}$, h_w) can be obtained from the following relationships which gives as a function of air mass velocity ($G_{a,h}$), and water mass velocity (L_w) (Zhani, 2013)

$$h_w = \frac{5900\, G_{a,h}^{0.5894}\, L_w^{0.169}}{A_h} \quad (23)$$

$$K_{a,h} = \frac{2.09\, G_{a,h}^{0.11515}\, L_w^{0.45}}{A_h} \quad (24)$$

$$h_{a,h} = k_{a,h}\, Cp_{a,h} \quad (25)$$

5.2. The dehumidifier

In the dehumidifier, indirect contact occurs between the hot humid air and the cooling water passing through condenser tubes. During dehumidification process, the air is cooled and dehumidified. The mathematical model can be formulated by applying the mass and heat balances according to Fig. 4.

Some assumptions were taken into consideration:

1- Dehumidification process is steady state conditions.
2- Corrugated condenser fins are simplified as flat fins.
3- Heat transfer between the medium and wall surface occurs only in radial direction.
4- Fouling resistance for inner and outer tube surfaces is neglected.

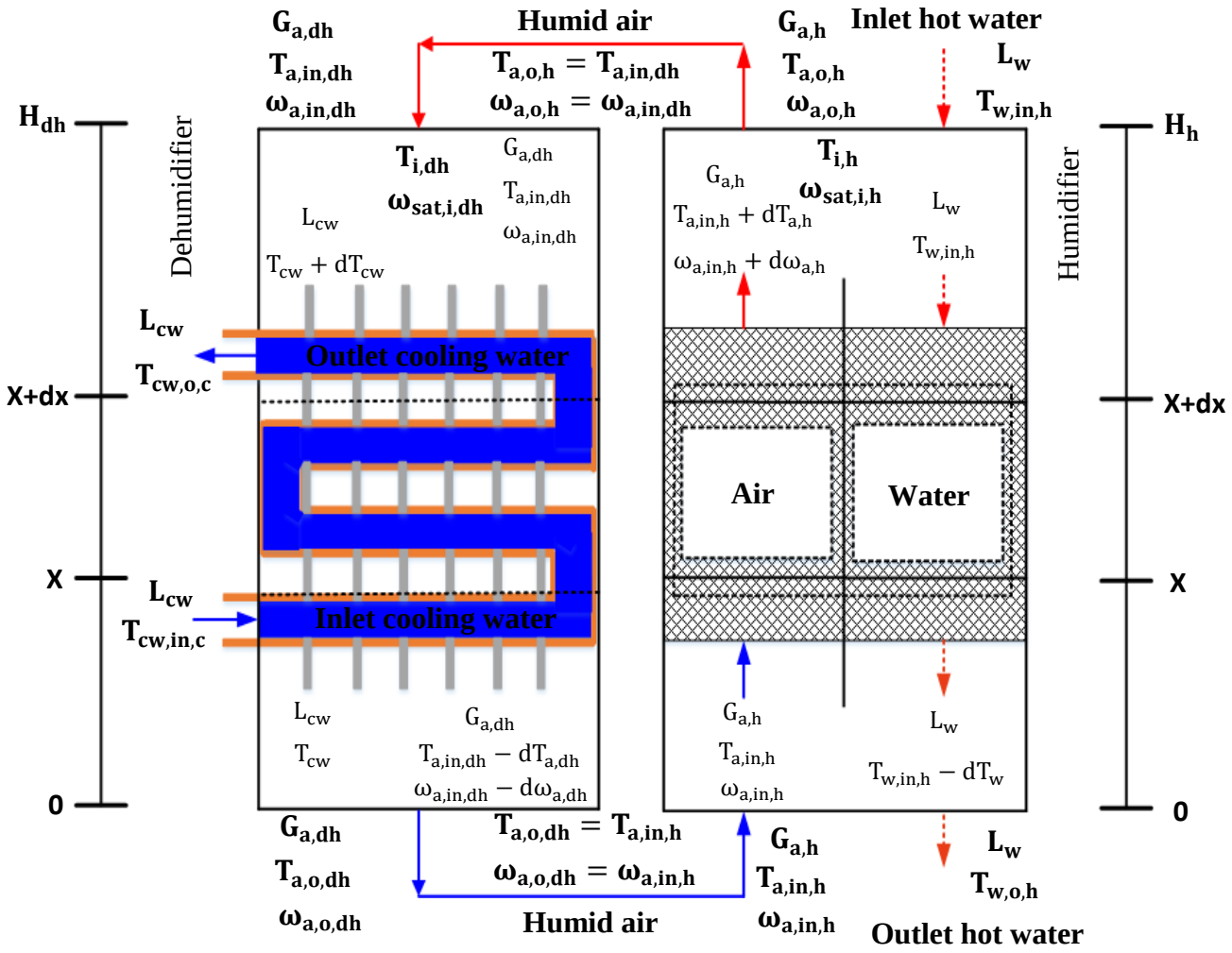

Fig. 4. Air and water flow direction for humidifier and dehumidifier with height dx.

Water phase heat balance; the heat energy transferred from the air water interface to the water-passing inside the condenser is equal to energy transferred by the water, as shown in Eq. (26).

$$UA_{dh}\left(T_{i,dh} - T_{cw,in,c}\right)dx = L_{cw}Cp_{cw}dT_{cw} \tag{26}$$

Eq. (26) can be rewritten as:

$$\frac{dT_{cw}}{dx} = \frac{UA_{dh}\left(T_{i,dh} - T_{cw,in,c}\right)}{L_{cw}Cp_{cw}} \tag{27}$$

Where U is condenser overall heat transfer coefficient (W/m^{2}K), A_{dh} is air water heat exchange area (m^2/m^3), $T_{i,dh}$ is temperature at air water interface (K), $T_{cw,in,c}$ is temperature of cooling water inlet to condenser (K), L_{cw} is cooling water mass velocity (kg/m^{2}s), Cp_{cw} is cooling water specific heat (J/kgK).

Air phase heat balance; the heat carried by the air is equal to sensible heat transmitted toward air water interface plus latent heat resulting from water vapor condensation transmitted to air water interface.

$$G_{a,dh}Cp_{a,dh}dT_{a,dh} = h_{a,dh}A_{dh}\left(T_{a,in,dh} - T_{i,dh}\right)dx + h_{fg}k_{a,dh}A_{dh}\left(\omega_{a,in,dh} - \omega_{sat,dh}\right)dx \quad (28)$$

Eq. (28) writes in another way:

$$\frac{dT_{a,dh}}{dx} = A_{dh}\left[\frac{h_{a,dh}\left(T_{a,in,dh} - T_{i,dh}\right) + h_{fg}K_{a,dh}\left(\omega_{a,in,dh} - \omega_{sat,dh}\right)}{G_{a,dh}Cp_{a,dh}}\right] \quad (29)$$

Where $h_{a,dh}$ is air film heat transfer coefficient (W/m^{2}K), $T_{a,in,dh}$is temperature of hot humid air inlet to dehumidifier (K), $K_{a,dh}$ is mass transfer coefficient at the interface (kg/m^{2}s), $Cp_{a,dh}$ is the air specific heat inside the dehumidifier (J/kgK).

Heat balance at vapor condensation interface; the cooling sensible heat of moist air received by vapor condensation interface plus latent heat liberated through condensation process at vapor condensate interface is equal to the heat transmitted from vapor condensate interface to cooling water, expressed by Eq. (30).

$$h_{a,dh}A_{dh}\left(T_{a,in,dh} - T_{i,dh}\right)dx + h_{fg}K_{a,dh}A_{dh}\left(\omega_{a,in,dh} - \omega_{sat,dh}\right)dx = UA_{dh}\left(T_{i,dh} - T_{cw,in,c}\right)dx \quad (30)$$

Eq. (30) is written in another way:

$$\omega_{sat,dh} = \frac{h_{a,dh}\left(T_{a,in,dh} - T_{i,dh}\right) + U\left(T_{cw,in,c} - T_{i,dh}\right)}{h_{fg}K_{a,dh}} + \omega_{a,in,dh} \quad (31)$$

The air saturation condition inside the dehumidifier ($\omega_{sat,dh}$) can be calculated using the equations that used in the humidifier, Eqs. (21, 22).

Mass balance at air condensate interface; the amount of water vapor that is condensed can be expressed by Eq. (32).

$$K_{a,dh}A_{dh}\left(\omega_{a,in,dh} - \omega_{sat,dh}\right)dx = G_{a,dh}d\omega_{a,dh} \quad (32)$$

Eq. (32) can be rewritten as:

$$\frac{d\omega_{a,dh}}{dx} = \frac{K_{a,dh}A_{dh}\left(\omega_{a,in,dh} - \omega_{sat,dh}\right)}{G_{a,dh}} \quad (33)$$

The overall heat transfer coefficient (U) is computed from Eq. (34):

$$U = \frac{1}{\frac{1}{h_{a,dh}} + \frac{1}{h_c} + \frac{\delta}{k_W} + \frac{1}{h_e}} \quad (34)$$

Air film heat transfer coefficient ($h_{a,dh}$) is calculated by Eq. (35) (Ben Bacha, 2013, Zhani and Ben Bacha, 2010).

$$h_{a,dh} = \frac{k_{a,dh}}{D_{h1}}0.35\left(\frac{P_t}{P_l}\right)^{0.2} Re^{0.6}\, pr^{0.36} \quad (35)$$

The mass transfer coefficient ($K_{a,dh}$) is determined using Lewis relation by Eq. (36) (Amer et al., 2009);

$$K_{a,dh} = \frac{h_{a,dh}}{Cp_{a,dh}} \tag{36}$$

The heat transfer coefficient of the condensate film (h_c) can be calculated by Nusselt relation in Eq. (37) (Robert et al., 1997);

$$h_c = 0.729 \left[\frac{\rho_{Fw}^2 \, g \, h_{fg} \, k_{Fw}^3}{\mu_{Fw} \, ND_{h2} \left(T_{i,dh} - T_W \right)} \right]^{0.25} \tag{37}$$

The heat transfer coefficient at interface of water condenser inside wall (h_e) is given by Eq. (38) (Amer et al., 2009);

$$h_e = \frac{k_{cw}}{D_{h2}} 0.032 \, Re^{0.8} \, pr^{0.33} \tag{38}$$

In the present study, the air passes in a closed cycle from the humidifier to the dehumidifier, and vice versa. Characteristics of the air leaving the humidifier are the same as those of the air entering the dehumidifier and vice versa. With known inlet air and water conditions, solving Eqs. (13, 15, 17, 27, 29, and 33) can give outlet air and water conditions. Engineering Equation Solver (EES) is used to solve the equations to obtain the required values after humidifier and dehumidifier chambers. Thus, it is possible to evaluate the performance indices of HDH water desalination system such as productivity ($\dot{m}_{Fw}$), gain output ratio (GOR) and thermal energy consumed ($\dot{Q}_S$), as shown in Fig. 5.

6. Results and Discussion

Several experiments have been conducted for HDH water desalination system using a closed-air cycle. Effect of different factors such as; air flow-rate, MR, and cooling water flow-rate on the performance indices has been studied. The performance indices include productivity, GOR, and the efficiency of the humidifier and dehumidifier. The desalinated water was evaluated economically. Finally, the experimental results are used to verify the theoretical values.

6.1. Effect of air flow-rate on the performance indices

Figure 6 shows the effect of the air flow-rate on productivity at humidifier water temperatures from 40 to 70 °C. The productivity increases with increasing the air flow-rate at all water temperatures. Increasing the air flow-rate during humidification process increases rate of vaporization from hot seawater per unit time and thus increases the fresh water condensation during the dehumidification process. Increasing the water temperature increases significantly the productivity with an average value of 1.46 kg/h, 2.59 kg/h, 4.40 kg/h, and 6.99 kg/h at water

temperatures of 40, 50, 60, and 70 °C, respectively. Increasing water temperature in humidifier makes air carry more water vapor, thus increases the fresh water productivity in the dehumidifier.

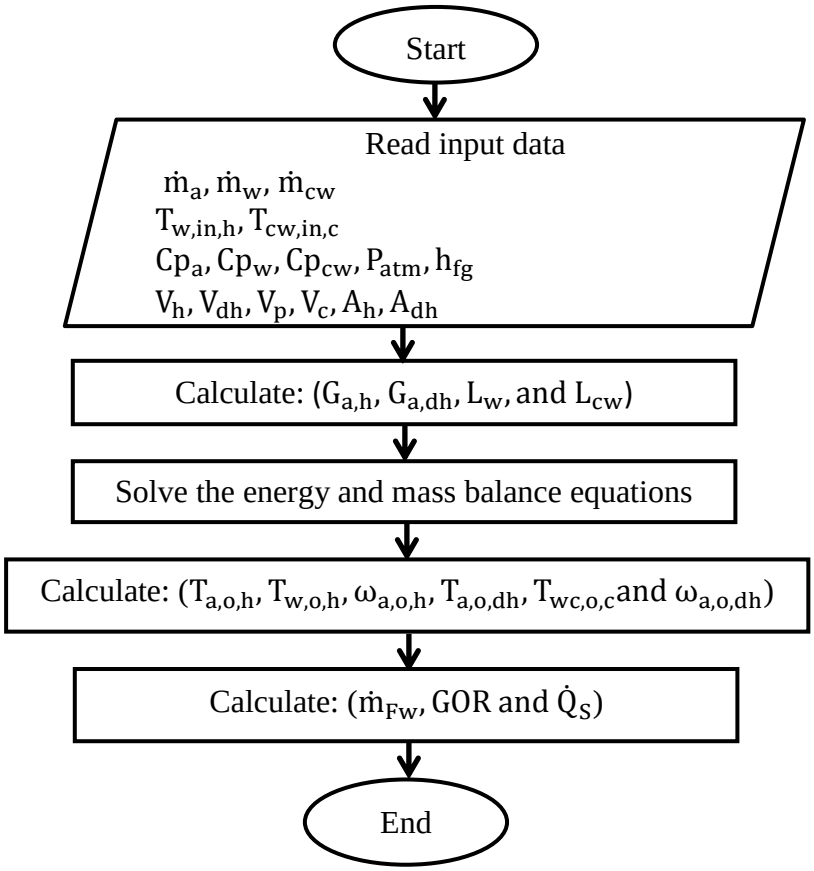

Fig. 5. Flow chart of the theoretical modeling.

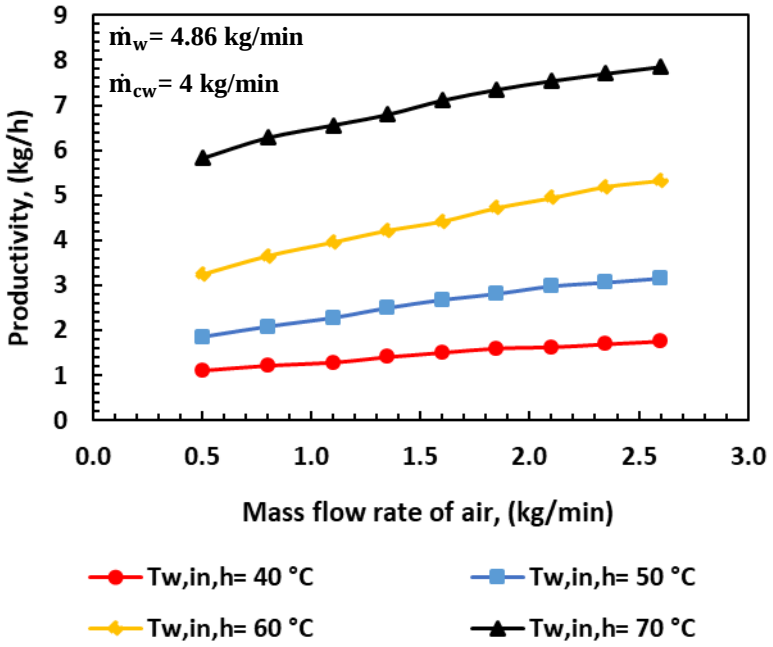

Fig. 6. Influence of mass flow-rate of air on the productivity.

Figure 7 shows GOR variation with air flow-rate at water temperatures from 40 to 70 °C. GOR of HDH desalination system decreases with increasing air flow-rate at all temperatures. With increasing mass flow-rate of air, hot water temperature decreases during humidification process. Thus, water temperature difference before and after the humidifier increases. Meanwhile, increasing energy input to HDH water desalination system is required to reheat water outlet from humidifier. According to Eq. (7), GOR of HDH system decreases with increasing air flow-rate. The figure shows that GOR increases with increasing water temperature. The average value of GOR is 0.71, 0.74, 0.78, and 0.81 at water temperatures of 40, 50, 60, and 70 °C, respectively. This shows that increasing the water temperature by 10 °C increases GOR by an average of 4.5%.

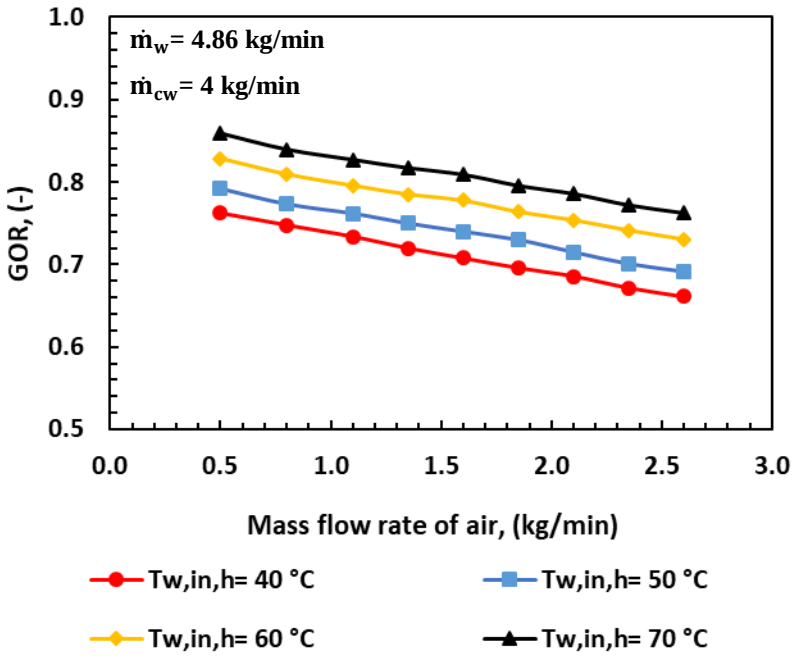

Fig. 7. Influence of air flow-rate on GOR.

The influence of air flow-rate on efficiency of humidifier and dehumidifier is shown in Fig. 8. Both of humidifier and dehumidifier efficiency follow an equivalent approach under the influence of air flow-rate, because increased air flow-rate decreases the efficiency of both humidifier and dehumidifier. The increasing of air flow-rate reduces contact time of air with the hot water within the humidifier and with cold surface of condenser within the dehumidifier. That results in reducing the air temperature after humidifier and increasing the air temperature after dehumidifier, which has a negative effect on the efficiency for both humidifier and dehumidifier.

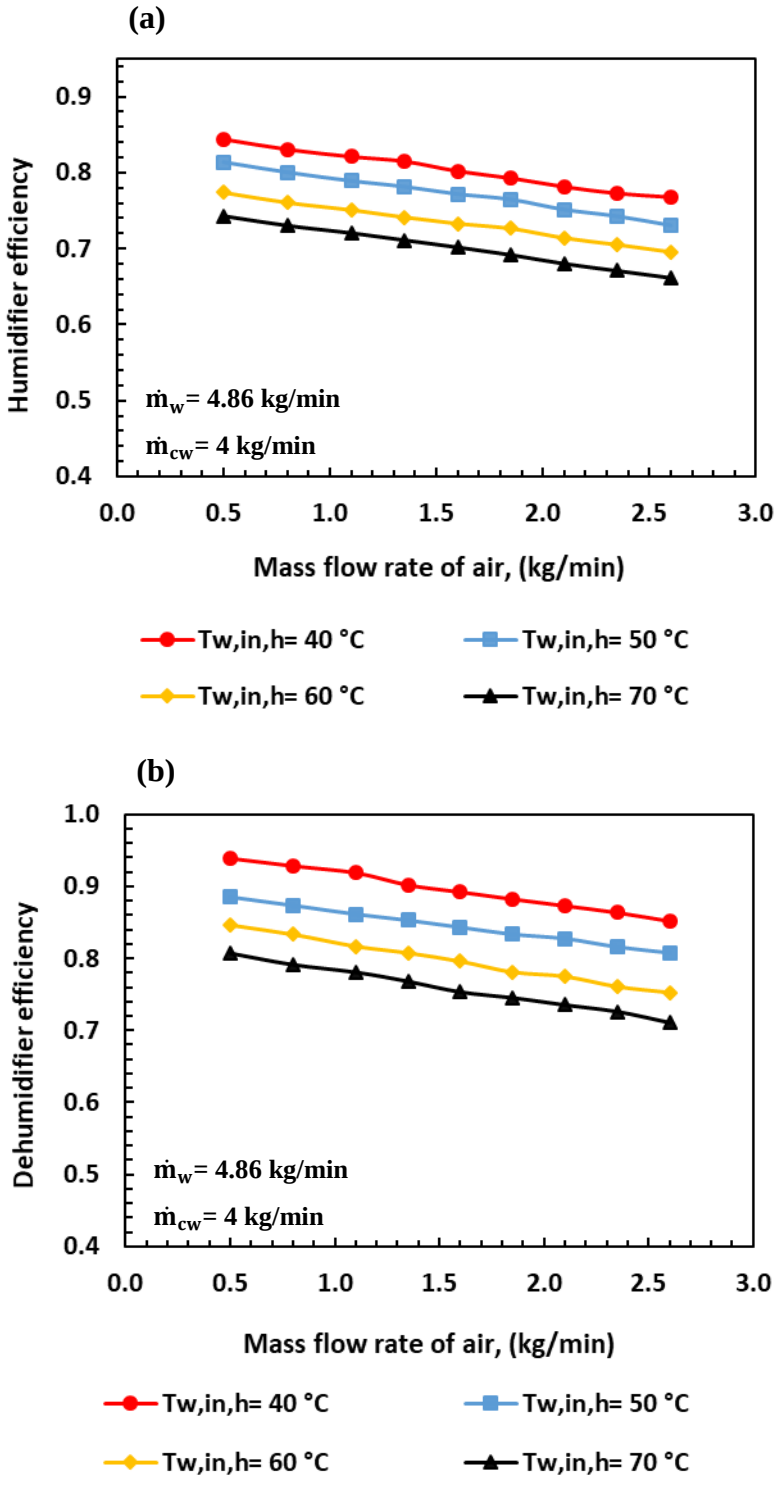

Fig. 8. Effect of the mass flow-rate of air on (a) humidifier efficiency, and (b) dehumidifier efficiency.

Figure 9 shows influence of air flow-rate on energy input to HDH desalination system at water temperatures from 40 to 70 °C. The energy consumption increases with increasing air flow-rate at all seawater temperatures. Increasing air flow-rate reduces the water temperature during the humidification process, and this requires an increase in energy needed to reheat the water outlet from humidifier to ensure the continuity of humidification cycle. Figure 9 illustrates that the energy input to the system increases as the water temperature rises. Average value of energy is 1.21 kW, 2.13 kW, 3.27 kW, and 5.03 kW at water temperature 40, 50, 60, and 70 °C, respectively. Increasing water temperature increases the energy exchanged with the air, thus increasing the thermal energy needed to reheat the water.

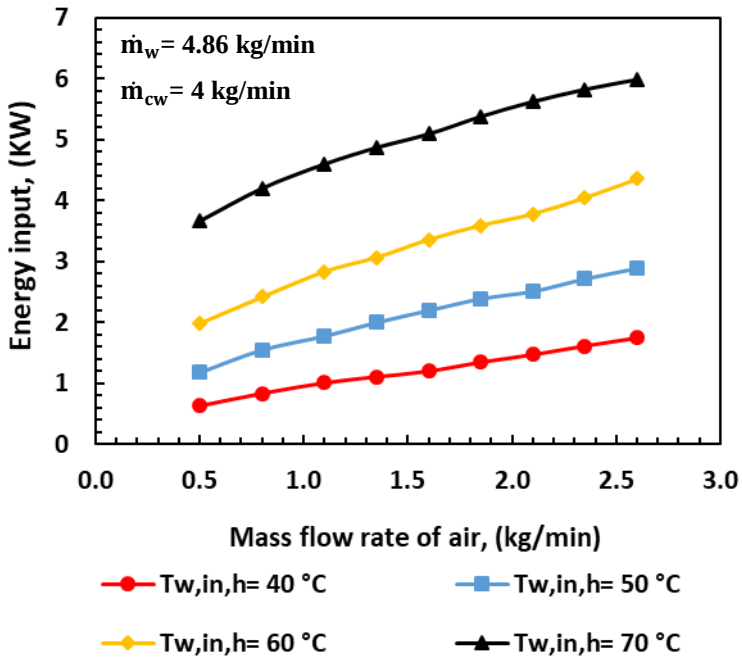

Fig. 9. Influence of air flow-rate on energy input to the desalination system.

6.2. Effect of mass flow-rate ratio on the performance indices

Productivity variation with MR at different water temperatures is shown in Fig. 10. At water temperature 40, 50, 60, and 70 °C, fresh water productivity clearly increases with increasing MR until the value of MR = 5, then the productivity slightly increases. Figure 10 is plotted with air flow-rate of 0.81 kg/min, thus MR increases due to an increase in water flow-rate, which leads to increasing water vapor carried by air inside the humidifier. As a result, the productivity increases during the dehumidification process. The figure shows also that increasing water temperature leads to increasing the productivity by an average of 1.04, 1.83, 3.39, and 5.49 kg/h at water temperature 40, 50, 60, and 70 °C, respectively.

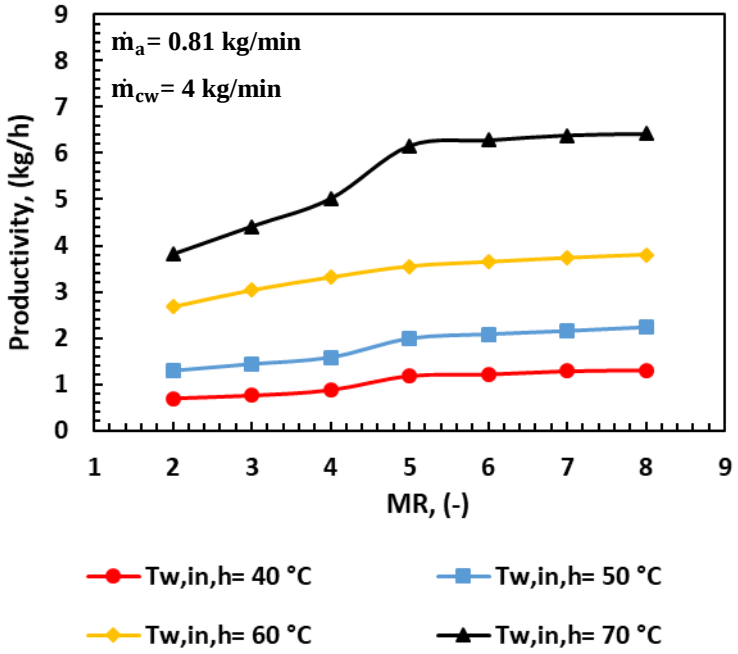

Fig. 10. Influence of the mass flow-rate ratio on the productivity.

Fig. 11 shows GOR variation with MR at water temperature 40, 50, 60, and 70 °C. GOR increases with increasing MR until value MR = 5, then the GOR begins to decrease as MR develops. GOR increases with rising the seawater temperature by an average of 0.73, 0.76, 0.79, and 0.82 at water temperatures of 40, 50, 60, and 70 °C, respectively. The results show also that the optimum MR is recorded 5 which achieves the maximum GOR = 0.86 at water temperature of 70 °C, as shown in Fig. 11 and a good productivity, as shown in Fig. 10. In the present work, at MR = 5, $\dot{m}_a$= 0.81 kg/min, and $T_{w,in,h}$= 70 °C, acceptable performance can be obtained from the HDH desalination system.

6.3. Effect of cooling water flow-rate on the performance indices

During dehumidification process, the influence of cooling water flow-rate on system efficiency is extremely important. Figure 12 shows the effect of the cooling water flow-rate on productivity and GOR. Increasing the flow-rate of cooling water leads to increasing the productivity and GOR. Increasing cooling water flow-rate decreases condenser surface temperature inside dehumidifier, resulting in increasing water vapor condensation. Maximum productivity and GOR values are 6.32 kg/h and 0.87 at cooling water flow-rate of 6 kg/min. Minimum productivity and GOR values are 5.52 kg/h and 0.83 at cooling water flow-rate 2 kg/min. Table 2 presents a summary of the experimental results.

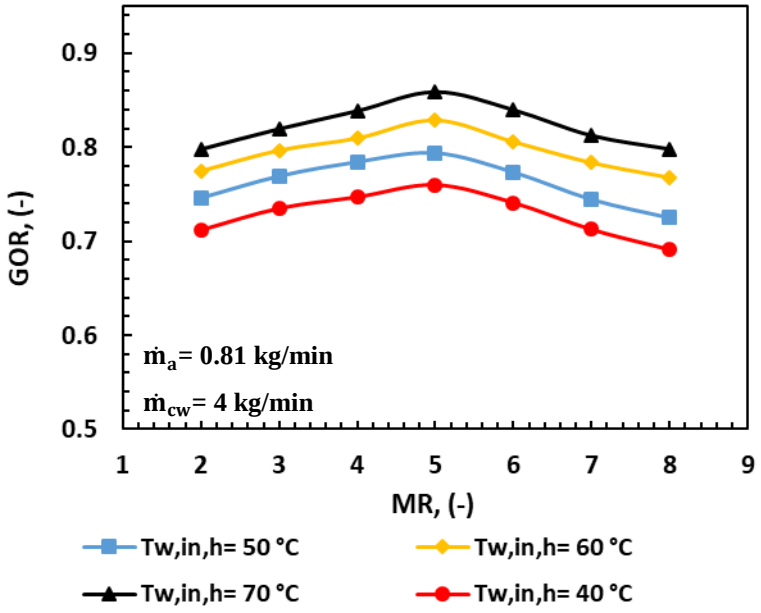

Fig. 11. Influence of mass flow-rate ratio on GOR.

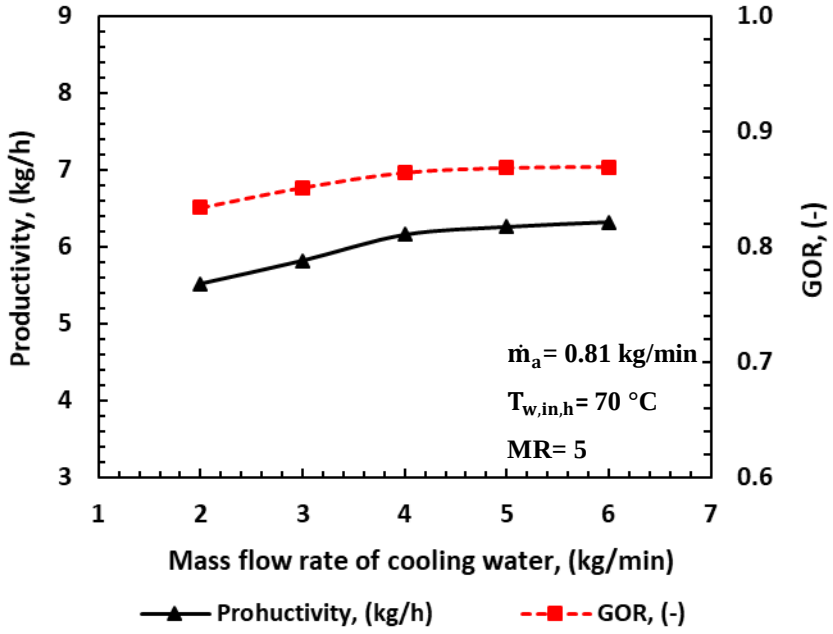

Fig. 12. Influence of cooling water flow-rate on productivity and GOR.

Table 2
Summary of the experimental results

Performance indices	Parameters effect	Average value			
		40°C	50°C	60°C	70°C
Productivity, (kg/h)	$\dot{m}_a$= 0.5-2.6 kg/min $T_{w,in,h}$= 40-70 °C $\dot{m}_{w,in,h}$= 4.86 kg/min $\dot{m}_{w,in,c}$= 4 kg/min	1.46 kg/h	2.59 kg/h	4.40 kg/h	6.99 kg/h
GOR, (-)	$\dot{m}_a$= 0.5-2.6 kg/min $T_{w,in,h}$= 40-70 °C $\dot{m}_{w,in,h}$= 4.86 kg/min $\dot{m}_{w,in,c}$= 4 kg/min	0.71	0.74	0.78	0.81
Humidifier efficiency, %	$\dot{m}_a$= 0.5-2.6 kg/min $T_{w,in,h}$= 40-70 °C $\dot{m}_{w,in,h}$= 4.86 kg/min $\dot{m}_{w,in,c}$= 4 kg/min	80 %	77 %	73 %	70 %
Dehumidifier efficiency, %	$\dot{m}_a$= 0.5-2.6 kg/min $T_{w,in,h}$= 40-70 °C $\dot{m}_{w,in,h}$= 4.86 kg/min $\dot{m}_{w,in,c}$= 4 kg/min	89 %	84 %	79 %	76 %
Energy input, (kW)	$\dot{m}_a$= 0.5-2.6 kg/min $T_{w,in,h}$= 40-70 °C $\dot{m}_{w,in,h}$= 4.86 kg/min $\dot{m}_{w,in,c}$= 4 kg/min	1.21 kW	2.13 kW	3.27 kW	5.03 kW
Productivity, (kg/h)	MR= 2-8 $\dot{m}_a$= 0.81 kg/min $T_{w,in,h}$= 40-70 °C $\dot{m}_{w,in,c}$= 4 kg/min	1.04 kg/h	1.83 kg/h	3.39 kg/h	5.49 kg/h
GOR, (-)	MR= 2-8 $\dot{m}_a$= 0.81 kg/min $T_{w,in,h}$= 40-70 °C $\dot{m}_{w,in,c}$= 4 kg/min	0.73	0.76	0.79	0.82
Productivity, (kg/h)	$\dot{m}_{w,in,c}$= 2-6 kg/min MR= 5	6.01 kg/h			
GOR, (-)	$\dot{m}_a$= 0.81 kg/min $T_{w,in,h}$= 70 °C	0.86			

6.4. Validation of the theoretical model

Validation of theoretical model is an important process for demonstrating the convergence between the theoretical values and the experimental results. The model is developed to obtain the results based on inputs under specific conditions of the system under study. However, the model results may have different validity levels. Accuracy of the values obtained from the theoretical model depends on its comparison with the experimental values. The error is determined by Eq. (39) (Nematollahi et al., 2013, Wu et al., 2017).

$$\varepsilon_{ar}(\%) = \frac{100}{k}\sum_{i=1}^{k}\frac{\left|T_{exp}(i) - T_{sim}(i)\right|}{T_{exp}(i)} \quad (39)$$

Where: k is measurements number, T_{exp} denotes the experimental data, and T_{sim} the model prediction.

In the current work, air and water temperature is recorded at many places within HDH desalination unit. Figure 13 shows the temperatures for the theoretical model and the experimental measurements. The average absolute difference are 7.2%, 2.16%, 3.95% and 2.81% for the air temperature before and after humidifier ($T_{a,in,h}$, $T_{a,o,h}$), water temperature after humidifier ($T_{w,o,h}$) and temperature of water leaving the condenser ($T_{cw,o,c}$), as illustrated in table 3. Based on the results, the outputs of the theoretical model are compatible with the experimental measurements. Fresh water productivity may be a performance index for any seawater desalination system. Figure 14 shows the mathematical and experimental fresh water productivity. Average absolute difference is found to be 5.92%. Good agreement is observed for calculated and experimental values.

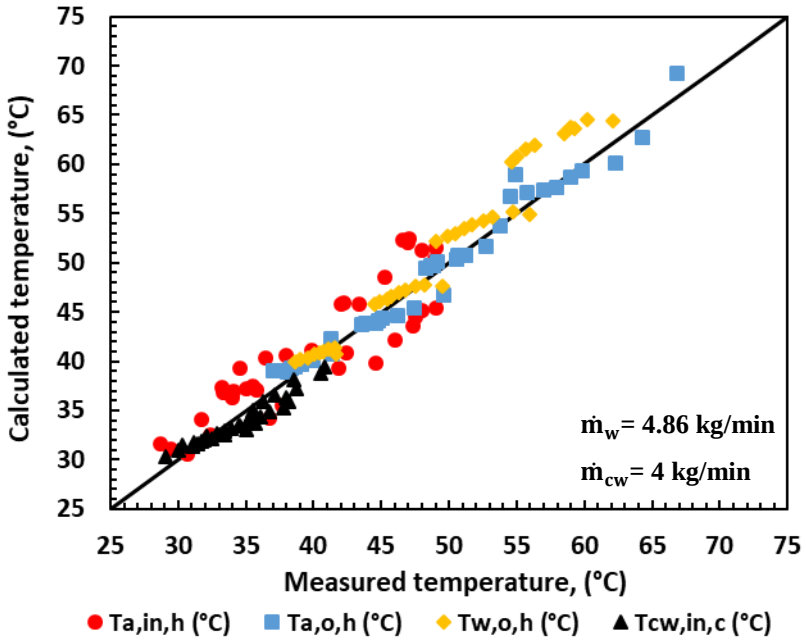

Fig. 13. Measured and theoretical temperatures of different places in desalination system.

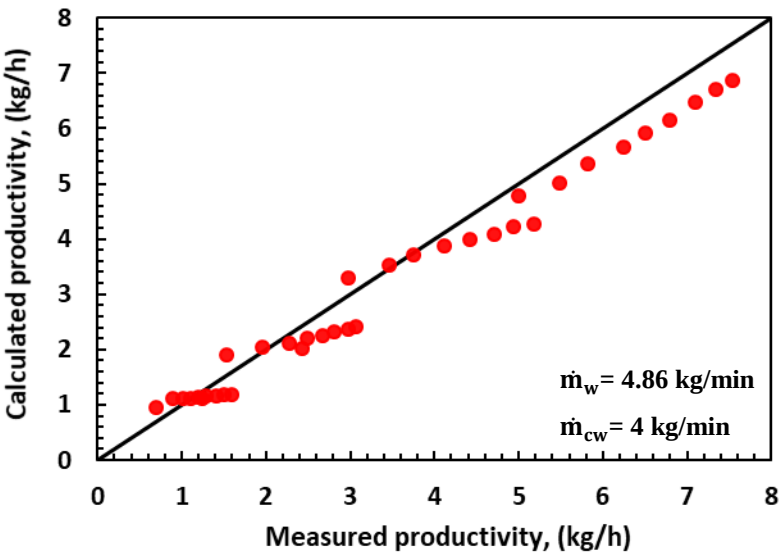

Fig. 14. Experimental and theoretical productivity of desalination system.

Table 3

The error percentage of model values.

Items	**Minimum error $\mathcal{E}_{min}$ (%)**	**Maximum error $\mathcal{E}_{max}$ (%)**	**Average error $\mathcal{E}_{av}$ (%)**
$T_{a,in,h}$	0.36	13.5	7.2
$T_{a,in,dh}$	0.06	7.17	2.16
$T_{w,o,h}$	0.14	10.56	3.95
$T_{cw,o,c}$	0.34	6.57	2.81
Productivity	1.30	10.35	5.92
Gain output ratio	0.15	9.53	2.54
Energy input	1.35	19.37	9.67

Solar thermal energy is the main driver of the HDH water desalination system. Figure 15 shows calculated data and experimental values for energy input to HDH water desalination system. Predicted energy has acceptable agreement with the experimental values. As shown in Fig. 15, the average absolute difference is 9.67%. GOR is an important index for water desalination unit, as it is an indicator of equilibrium between the productivity and the energy consumed. Fig. 16 shows a comparison between the predicted values and experimental results of GOR. The figure reflects the great similarity between the theoretical and measured values, at an average value of 2.54 %.

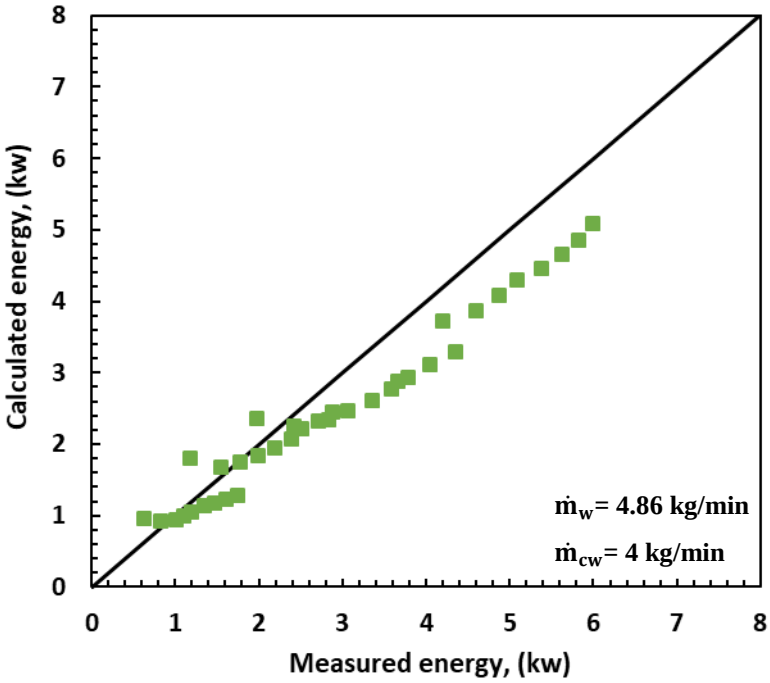

Fig. 15. Experimental and theoretical energy input to desalination system.

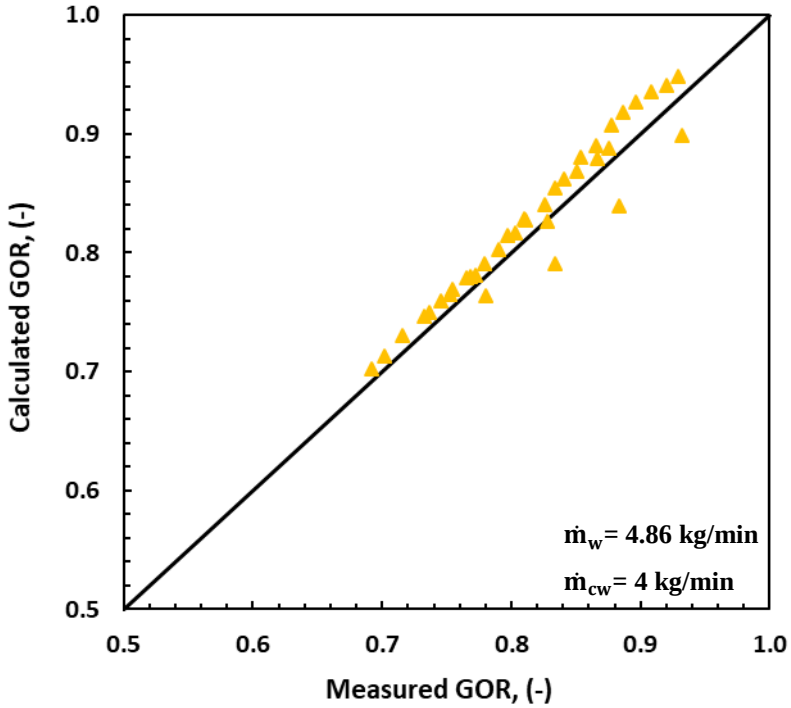

Fig. 16. Experimental and theoretical GOR of desalination system.

7. Econemic evaluation

The economic study is extremely important to calculate the cost of producing fresh water and thus evaluate the desalination system. Many researchers have conducted studies for calculating the cost of fresh water production (El-Agouz, 2010, Kabeel et al., 2010, Zhang et al., 2018). Therefore,

the current study has estimated the cost of producing one liter of fresh water using the following steps;

The total fixed cost (F) for HDH desalination unit is estimated of 1052 US$. The details are illustrated in table 4.

Eq. (40) is used to determine the capital recovery factor (CRF).

$$\mathrm{CRF} = \frac{\mathrm{i}\,(1+\mathrm{i})^{\mathrm{n}}}{(1+\mathrm{i})^{\mathrm{n}}-1} \tag{40}$$

Where: i is interest rate (%), where it can be assumed of 12%, and n is life year's number, where it can be assumed of 10 years.

Eq. (41) is used to determine the fixed annual cost (FAC).

$$\mathrm{FAC} = \mathrm{F} \times \mathrm{CRF} \tag{41}$$

Sinking fund factor (SFF) is calculated using Eq. (42).

$$\mathrm{SFF} = \frac{\mathrm{i}}{(1+\mathrm{i})^{\mathrm{n}}-1} \tag{42}$$

The salvage value of HDH desalination system (S) can be assumed of 20% from the unit total cost, as written in Eq. (43):

$$\mathrm{S} = 0.2 \times \mathrm{F} \tag{43}$$

Eq. (44) is used to calculate the annual salvage value (ASV).

$$\mathrm{ASV} = \mathrm{SFF} \times \mathrm{S} \tag{44}$$

The annual maintenance cost (AMC) can be assumed of 15% of the fixed annual cost, as written in Eq. (45):

$$\mathrm{AMC} = 0.15 \times \mathrm{FAC} \tag{45}$$

Eq. (46) is used to calculate the total annual running cost (AC).

$$\mathrm{AC} = \mathrm{FAC} + \mathrm{AMC} - \mathrm{ASV} \tag{46}$$

The cost of producing one liter of fresh water (CPL) can be determined by the ratio between total annual cost (AC) and total annual productivity (M), as expressed in Eq. (47):

$$\mathrm{CPL} = \frac{\mathrm{AC}}{\mathrm{M}} \tag{47}$$

The annual productivity of HDH desalination system obtained at water temperature of 70 °C inside the humidifier is found to be 16744.32 L/year.The daily period of running the desalination system is 8 h/day; (from 9 AM to 5 PM). HDH desalination system is assumed to operate 340 days/year as Egypt is characterized by the sunshine throughout the year (Hamed et al., 2015, Mohamed et al., 2020). The cost of producing one liter of desalinated water by the proposed system is 0.012 US$/L.

Table 4
Approximate cost of the HDH devices.

Devices	**The cost**
Humidifier and dehumidifier chambers	92US$
Ducts	61US$
Storage tank	62US$
Heat exchanger	65US$
Metal stands	60US$
Water pump	120 US$
Air fan	125US$
Evacuated tube collector	300US$
Structure packing	62US$
Insulation-materials	35US$
Valves and pipelines	70US$
Total cost	1052US$

Table 5 illustrates a comparison of the current study with some previous works. The table illustrates some of the important components and results of the desalination system such as packing type, and productivity. The table illustrates some available parameters and results such as packing material, and productivity. In addition, the table shows the production cost per liter of desalinated water. Based on available data by table 5, it can be concluded that the proposed desalination system works effectively compared to some of the previous works. Besides, the cost for producing desalinated water is low, compared with previous researches.

Table 5
Comparison of the current study with some previous works.

Reference	**Packing material**	**Productivity (L/h)**	**Cost (US$/L)**
Zhang et al. (2018)	Polypropylene	22.26	0.051
Hamed et al. (2015)	Cellulose paper	5.5	0.0578
Faegh and Shafii (2019)	CF1200MA Cross Fluted Film Fill Media	0.91	0.014
Xu et al. (2018)	Honeycomb paper	12.75	0.042
Dehghani et al. (2019)	Polypropylene	4.9	-
Hermosillo et al. (2012)	Cellulose paper	1.45	-
Elminshawy et al. (2015)	-	-	0.035
Rajaseenivasan and Srithar (2017)	-	6.1	0.0133
Deniz and Çınar (2016)	Cellulose paper	1.12	0.0981
Current study	Cellulose paper	6.16	0.012

8. Conclusions

In recent decades, the desalination process has become extremely important for many regions. HDH water desalination system is a promising solution for many areas. In this study, solar HDH water desalination system based on a closed air cycle is established and its results are compared with calculated values. Effect of parameters on productivity, gain output ratio, humidifier efficiency, and dehumidifier efficiency are investigated. The parameters include the air flow-rate, mass flow-rate ratio, and cooling water flow-rate. Experiments have been conducted at water temperature 40, 50, 60, and 70 °C. An economic evaluation of the desalinated water production has been also conducted. The results show that increasing air flow-rate leads to increasing water productivity, while it reduces GOR, humidifier efficiency, and dehumidifier efficiency. In addition, increasing air flow-rate requires increasing the energy needed to operate the desalination unit. At water temperature range from 40 to 70 °C, an increase in water temperature by 10 °C leads to increase of fresh water production with an average 69 %. GOR and productivity increase with increasing mass flow-rate ratio. The results show also that the optimum MR is recorded 5 which achieves the maximum GOR = 0.86 with temperature of water 70 °C. Further, increasing cooling water flow-rate increases both productivity and GOR. Maximum productivity and GOR values are 6.32 kg/h and 0.87 at cooling water flow-rate 6 kg/min. The cost of producing one liter of potable water is 0.012US$. The results of theoretical model are good compared to the experimental results.

References

Amer, E. H., H. Kotb, G. H. Mostafa, and A. R. El-Ghalban. 2009. Theoretical and experimental investigation of humidification-dehumidification desalination unit. Desalination 249(3): 949–59.

Ben Bacha, Habib. 2013. Dynamic modeling and experimental validation of a water desalination prototype by solar energy using humidification dehumidification process."Desalination 322: 182–208.

Conde, M. 2007. Thermophysical properties of humid air - models and background. Engineering, Zurich.

Dehghani, Saeed, Abhijit Date, and Aliakbar Akbarzadeh. 2019. An experimental study of brine recirculation in humidification-dehumidification desalination of seawater. Case Studies in Thermal Engineering 14(December 2018).

Deniz, Emrah, and Serkan Çınar. 2016. Energy, exergy, economic and environmental (4E) analysis of a solar desalination system with humidification-dehumidification. Energy Conversion and Management 126: 12–19.

El-Agouz, S. A. 2010. Desalination based on humidification-dehumidification by air bubbles passing through brackish water. Chemical Engineering Journal 165(2): 413–19.

Elminshawy, Nabil A.S., Farooq R. Siddiqui, and Mohammad F. Addas. 2015. Experimental and analytical study on productivity augmentation of a novel solar humidification-dehumidification (HDH) system. Desalination 365: 36–45.

Faegh, Meysam, and Mohammad Behshad Shafii. 2019. Performance evaluation of a novel compact humidification-dehumidification desalination system coupled with a heat pump for design and off-design conditions. Energy Conversion and Management 194(February): 160–72.

A. Fouda, S. A. Nada, H. F. Elattar, S. Rubaiee, and A. Al-Zahrani. 2018. "Performance analysis of proposed solar HDH water desalination systems for hot and humid climate cities. Applied Thermal Engineering 144(July): 81–95.

Gao, Penghui, Lixi Zhang, and Hefei Zhang. 2008. Performance analysis of a new type desalination unit of heat pump with humidification and dehumidification. Desalination 220(1–3): 531–37.

H. Robert, W. Perry Donald Green, Don Green. 1997. *Chemical Engineers' Hand- Book*. Seventh ed. McGraw-Hill Professional.

Hamed, Mofreh H, A E Kabeel, Z M Omara, and S W Sharshir. 2015. Mathematical and experimental investigation of a solar humidification – dehumidification desalination unit. Desalination 358: 9–17.

Hermosillo, Juan Jorge, Camilo A. Arancibia-Bulnes, and Claudio A. Estrada. 2012. Water desalination by air humidification: mathematical model and experimental study. Solar Energy 86(4): 1070–76.

Hou, Shaobo, and Hefei Zhang. 2008. A Hybrid solar desalination process of the multi-effect humidification dehumidification and basin-type unit. Desalination 220: 552–57.

Kabeel, A. E., A. M. Hamed, and S. A. El-Agouz. 2010. Cost analysis of different solar still configurations. Energy 35(7): 2901–8.

Kabeel, A. E., Mofreh H. Hamed, Z. M. Omara, and S. W. Sharshir. 2013. Water desalination using a humidification-dehumidification technique—A Detailed Review. Natural Resources 04(03): 286–305.

A. E. Kabeel, M. H. Hamed, Z. M. Omara, and S. W. Sharshir. 2014. Experimental study of a humidification-dehumidification solar technique by natural and forced air circulation. Energy 68: 218–28.

Kalogirou, Soteris A. 2005. Seawater desalination using renewable energy sources. Progress in Energy and Combustion Science 31(3): 242–81.

Kasamsetty, K. Sai, and Benny Raphael. 2018. Performance evaluation of a high-influx, bubble dehumidifier. Energy and Buildings 173: 291–301.

Mohamed, A S A, M Salem Ahmed, and Abanob G Shahdy. 2020. Theoretical and experimental study of a seawater desalination system based on humidification-dehumidification technique. Renewable energy 152: 823–34.

Nafey, A. S., H. E.S. Fath, S. O. El-Helaby, and A. Soliman. 2004a. Solar desalination using humidification-dehumidification processes. part II. An experimental investigation. Energy Conversion and Management 45(7–8): 1263–77.

Nafey, A. S., H. E.S. Fath, S. O. El-Helaby, and A. M. Soliman. 2004b. Solar desalination using humidification dehumidification processes. part I. A numerical investigation. Energy Conversion and Management 45(7–8): 1243–61.

Nematollahi, Farhad, Amir Rahimi, and Touraj Tavakoli Gheinani. 2013. Experimental and theoretical Energy and exergy analysis for a solar desalination system. *Desalination* 317: 23–31.

Patel, Anil M, H S Chokshi, and Mandar M Sumant. 2014. A Review of circular solar collector for close- water , open-air (CWOA) air heated humidification and dehumidification process. Journal of Basic and Applied Engineering Research 1(9): 10–16.

Rahbar, N., and J. A. Esfahani. 2012. Experimental study of a novel portable solar still by utilizing the heatpipe and thermoelectric module. Desalination 284: 55–61.

Rajaseenivasan, T., R. K. Shanmugam, V. M. Hareesh, and K. Srithar. 2016. Combined probation of bubble column humidification dehumidification desalination system using solar collectors. Energy 116: 459–69.

Rajaseenivasan, T., and K. Srithar. 2017. An Investigation into a laboratory scale bubble column humidification dehumidification desalination system powered by biomass energy. Energy Conversion and Management 139: 232–44.

Sharqawy, Mostafa H., John H. Lienhard V, and Syed M. Zubair. 2010. Thermophysical properties of seawater: A review of existing correlations and data. Desalination and Water Treatment 16(1–3): 354–80.

Sharqawy, Mostafa H, Mohamed A Antar, Syed M Zubair, and Abubaker M Elbashir. 2014. Optimum thermal design of humidification dehumidification desalination systems. Desalination 349: 10–21.

Sharshir, S W et al. 2016. A Hybrid desalination system using humidification-dehumidification and solar stills integrated with evacuated solar water heater. Energy Conversion and Management 124: 287–96.

K. Srithar, T. Rajaseenivasan, M. Arulmani, R. Gnanavel, M. Vivar, and M. Fuentes. 2018. Energy recovery from a vapour compression refrigeration system using humidification dehumidification desalination. Desalination 439(March): 155–61.

G. Wu, H. Zheng, X. Ma, C. Kutlu, and Y. Su. 2017. Experimental investigation of a multi-stage humidification-dehumidification desalination system heated directly by a cylindrical Fresnel lens solar concentrator. Energy Conversion and Management 143: 241–51.

Wu, Gang, Hong Fei Zheng, Fei Wang, and Ze Hui Chang. 2017. Parametric study of a tandem desalination system based on humidification-dehumidification process with 3-stage heat recovery. Applied Thermal Engineering 112: 190–200.

Xu, H., Y. Zhao, T. Jia, and Y. J. Dai. 2018. Experimental investigation on a solar assisted heat pump desalination system with humidification-dehumidification. Desalination 437(March): 89–99.

Yildirim, Cihan, and Ismail Solmuş. 2014. A Parametric study on a humidification-dehumidification (HDH) desalination unit powered by solar air and water heaters. Energy Conversion and Management 86: 568–575.

Y. Zhang, C. Zhu, H. Zhang, W. Zheng, S. You, and Y. Zhen. 2018. Experimental study of a humidification-dehumidification desalination system with heat pump unit. Desalination 442(January): 108–17.

Zhani, Khalifa. 2013. Solar desalination based on multiple effect humidification process: Thermal performance and experimental validation. Renewable and Sustainable Energy Reviews 24: 406–17.

Zhani, Khalifa, and Habib Ben Bacha. 2010. Modeling and simulation of a new design of the SMCEC desalination unit using solar energy. Desalination and Water Treatment 21(1–3): 346–56.